Available online at www.sciencedirect.com
ScienceDirect
Journal of Catalysis 255 (2008) 20–28
JOURNAL OF CATALYSIS
www.elsevier.com/locate/jcat

A density functional theory study of the α-olefin selectivity in Fischer–Tropsch synthesis

Jun Cheng [a], Tao Song [a], P. Hu [a,*], C. Martin Lok [b], Peter Ellis [c], Sam French [c]

[a] *School of Chemistry, The Queen's University of Belfast, Belfast, BT9 5AG, UK*
[b] *Johnson Matthey Technology Centre, Billingham Cleveland, TS23 1LB, UK*
[c] *Johnson Matthey Technology Centre, Reading, RG4 9NH, UK*

Received 9 October 2007; revised 20 December 2007; accepted 17 January 2008

Abstract

We studied the α-olefin selectivity in Fischer–Tropsch (FT) synthesis using density functional theory (DFT) calculations. We calculated the relevant elementary steps from C_2 to C_6 species. Our results showed that the barriers of hydrogenation and dehydrogenation reactions were constant with different chain lengths, and the chemisorption energies of α-olefins from DFT calculations also were very similar, except for C_2 species. A simple expression of the paraffin/olefin ratio was obtained based on a kinetic model. Combining the expression of the paraffin/olefin ratio and our calculation results, experimental findings are satisfactorily explained. We found that the physical origin of the chain length dependence of paraffin/olefin ratio is the chain length dependence of both the van der Waals interaction between adsorbed α-olefins and metal surfaces and the entropy difference between adsorbed and gaseous α-olefins, and that the greater chemisorption energy of ethylene is the main reason for the abnormal ethane/ethylene ratio.

Keywords: Fischer–Tropsch; DFT; Co; α-Olefin selectivity; Van der Waals; Entropy

1. Introduction

Reactivity and selectivity are two fundamental issues in catalysis. Very often, selectivity is considered more important to real chemical industries. Whereas reactivity has been extensively investigated and great progress has been made, the theoretical understanding of selectivity in heterogeneous catalysis still falls short of chemists' expectations. In the work reported here, we investigated the α-olefin selectivity in Fischer–Tropsch (FT) synthesis [1–8] using density functional theory (DFT) calculations.

FT synthesis, which converts synthesis gas (CO and H_2) to various long-chain hydrocarbons (mainly *n*-paraffins and α-olefins), provides an alternative route to produce fuels and petrochemicals [9–15] as the global reserves of crude oil are being exhausted. Much experimental [16–22] and theoretical [23–28] work has been dedicated to FT synthesis because of its importance, and some significant achievements have been made. The general consensus regarding the FT mechanism is as follows: (i) CO and H_2 dissociate on metal surfaces; (ii) O is removed via water formation, and C is hydrogenated to CH_x ($x = 1$–3); (iii) carbon chains are prolonged via stepwise polymerization; and (iv) carbon chains are terminated by β-hydrogen elimination, yielding α-olefins or by α-hydrogenation producing *n*-paraffins. *n*-Paraffins are not reactive under typical FT conditions, whereas α-olefins are able to readsorb and subsequently to undergo hydrogenation to produce *n*-paraffins or reinsert into chain growth reactions.

α-Olefin selectivity (which is usually measured by the paraffin/olefin (P/O) ratio, a fundamental issue in FT synthesis) remains elusive, however. Linear α-olefins are high-value products in the FT process that are widely used commercially in, for example, polymers, additives, and specialty chemicals [29]. Improving α-olefin selectivity will result in great economic benefits in FT technology [8]. Although much effort has been devoted to this issue [30–38], which factors predominately determine α-olefin selectivity remains unclear.

* Corresponding author. Fax: +44 (0) 28 9097 4687.
E-mail address: p.hu@qub.ac.uk (P. Hu).

0021-9517/$ – see front matter
doi:10.1016/j.jcat.2008.01.027

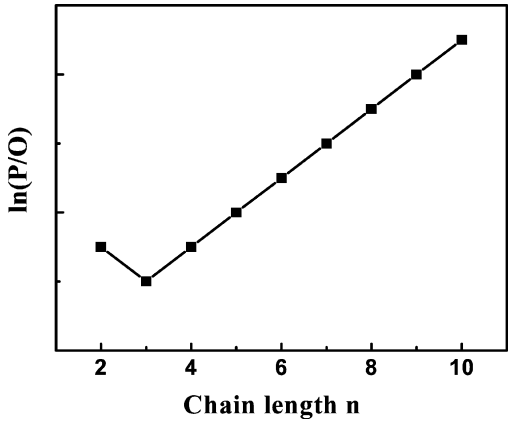

Fig. 1. Schematic illustration of the chain length dependence of P/O ratio in FT synthesis.

Experimentally, two interesting features about α-olefin selectivity haven been identified (Fig. 1) [31,33]: (i) the P/O ratio generally increases exponentially with chain length $n > 2$, and (ii) when the chain length is 2, the P/O ratio deviates significantly from the curve. The chain length dependence of the P/O ratio can be expressed in the following equation, with chain length $n > 2$:

$$\frac{P_n}{O_n} \propto e^{cn} \tag{1}$$

where c is a constant. To date, three models have been suggested to explain the α-olefin selectivity: (i) the chain length-dependent solubility in FT wax [34,35], (ii) the chain length-dependent diffusion limitation [36–38], and (iii) the chain length-dependent preferential physisorption [31]. Experimental evidence [31] has shown that in the absence of a wax layer over the catalyst surfaces, the P/O ratio still increased exponentially with the chain length, demonstrating that solubility and diffusion limitation are simply influencing factors, rather than the physical origin of the chain length dependence of the P/O ratio. It also is unlikely that the transfer of α-olefins from the precursor state (physisorption) to the chemisorbed state is kinetically important, due to the fact that the transfer processes must be much faster than the surface reactions. Thus, the preferential physisorption also may not be the reason for the chain length-dependent P/O ratio. Perhaps more importantly, to date no model can explain the abnormal ethane/ethylene ratio. Consequently, the physical origin of the α-olefin selectivity remains unclear. Gaining insight into the chain length-dependent P/O ratio and clues as to how to best improve the α-olefin selectivity in FT synthesis are highly desirable goals.

In the work reported in this paper, we investigated α-olefin selectivity in FT synthesis using DFT calculations. Our goal was to obtain a simple expression to describe the α-olefin selectivity in FT synthesis, aiming to explain why the P/O ratio increases exponentially with chain length after C_2 and why the ratio of C_2 is erratic. Moreover, we explored some ways to improve the α-olefin selectivity.

The paper is organized as follows. We describe our calculation method in Section 2. In Section 3, we discuss the chemisorption of n-alkyl groups and 1-alkenes and present the barriers of n-alkyl hydrogenation and dehydrogenation. In Section 4, we use a kinetic model to analyze our DFT results to explain the chain length dependence of the P/O ratio. We summarize our conclusions in Section 5.

2. Methods

In this work, the SIESTA code [39] with Troullier–Martins norm-conserving scalar relativistic pseudopotentials [40] was used, along with a double-zeta plus polarization (DZP) basis set. The localization radii of the basis functions were determined from an energy shift of 0.01 eV. A standard DFT supercell approach with the Perdew–Burke–Ernzerhof (PBE) form of the generalized gradient approximation (GGA) functional [41] was implemented with a mesh cutoff of 200 Ry. Spin polarization was included in the calculations.

All reactions were simulated on flat Co(0001). In the calculations, the surface was modeled by four layers of metals, and the vacuum space of the unit cell was varied with the chain length of the adsorbate to keep the distance between the top of adsorbate and the bottom layer in the unit cell above at around 10 Å. A p(3×2) unit cell and surface Monkhorst Pack meshes of $3 \times 4 \times 1$ k-point sampling in the surface Brillouin zone were used. The bottom two layers of metal atoms were fixed, and the top two layers and the adsorbates were relaxed.

The transition states (TSs) were searched using a constrained optimization scheme [42–44]. The distance between the reactants was constrained at an estimated value, and the total energy of the system was minimized with respect to all the other degrees of freedom. The TSs could be located via changing the fixed distance and were confirmed by two rules: (i) all forces on atoms vanish, and (ii) the total energy is maximum along the reaction coordinate but minimum with respect to the remaining degrees of freedom.

3. Results

To gain insight into the origin of the chain length dependence of the P/O ratio, we calculated the hydrogenation and dehydrogenation reactions of n-alkyl groups on Co(0001). The most stable structures of n-alkyl group adsorbed on Co(0001) as well as 1-alkene and H were calculated and considered the initial states (ISs). Based on the IS structures, the transition states (TSs) in n-alkyl hydrogenation and dehydrogenation were located. To unveil the trend of calculated results with different chain lengths, we computed these reactions from C_2 up to C_6 species.

3.1. Chemisorption of n-alkyl groups and 1-alkenes on Co(0001)

Because adsorbed n-C_nH_{2n+1} and 1-C_nH_{2n} are involved in the hydrogenation and dehydrogenation of n-alkyl groups, we first studied the chemisorption of n-C_nH_{2n+1} and 1-C_nH_{2n} with the chain length n of 2 to 6 on Co(0001). Figs. 2a–2f show the most stable structures of n-alkyl groups located on the hcp hollow sites with the carbon chain upright over the Co surface

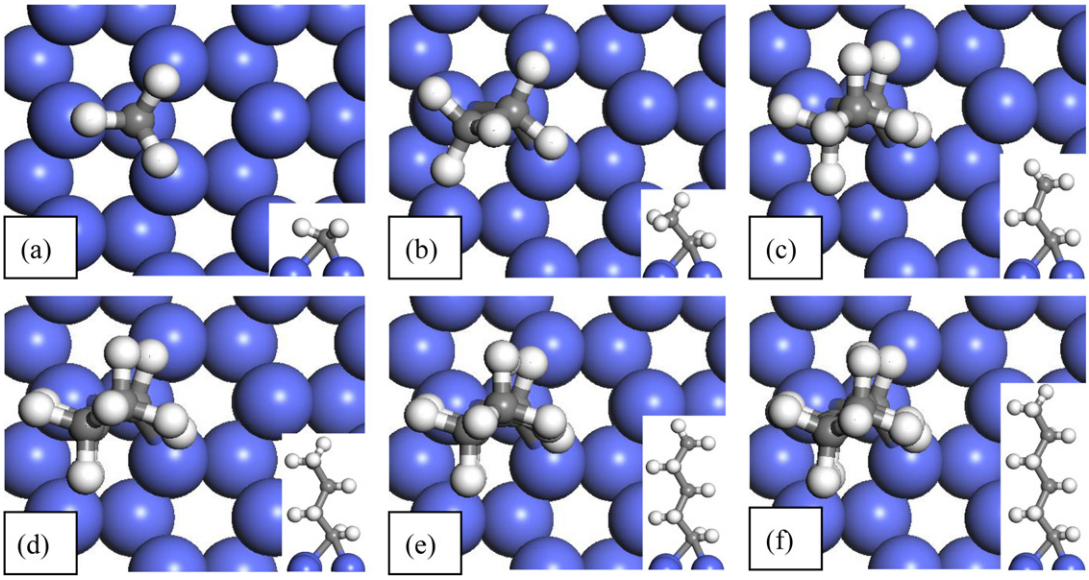

Fig. 2. Top view and side view (inserted) of the structures of adsorbed n-alkyl groups on Co(0001): (a) methyl; (b) ethyl; (c) n-propyl; (d) n-butyl; (e) n-pentyl; (f) n-hexyl. The white balls are H atoms, the gray balls are C atoms and the blue balls are Co atoms. This notation is used throughout this paper. (For interpretation of the references to color in this figure legend, the reader is referred to the web version of this article.)

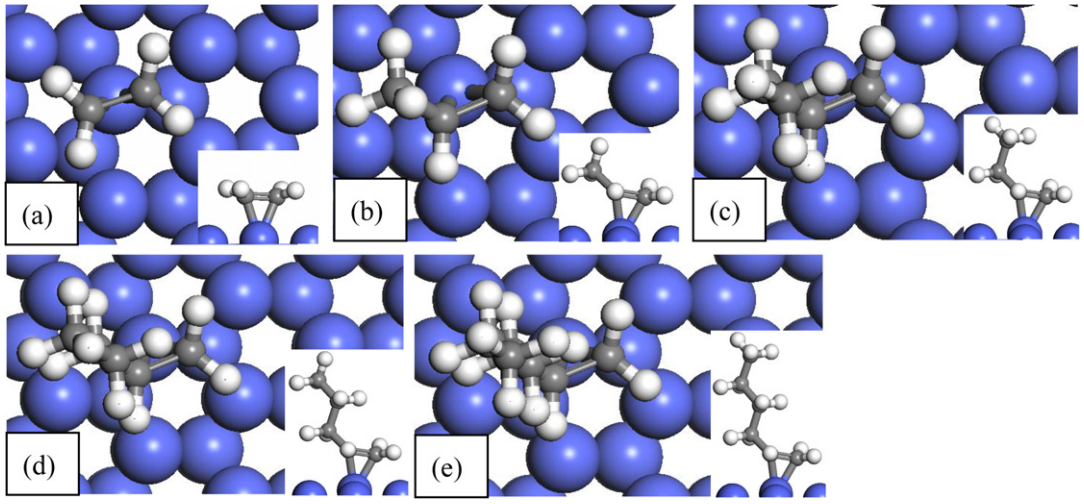

Fig. 3. Top view and side view (inserted) of the structures of adsorbed 1-alkenes on Co(0001): (a) ethylene; (b) propene; (c) 1-butene; (d) 1-pentene; (e) 1-hexene.

Table 1
Structural parameters and DFT chemisorption energies of adsorbed n-alkyl groups

Chain length n	$d_{C–Co}$ (Å)	Chem. energy (eV)
1	2.168, 2.131, 2.122	2.00
2	2.182, 2.201, 2.328	1.60
3	2.200, 2.244, 2.337	1.62
4	2.176, 2.236, 2.378	1.60
5	2.174, 2.235, 2.379	1.60
6	2.173, 2.232, 2.375	1.62

$d_{C–Co}$ are the distances between the unsaturated C atom and the nearest three Co atoms.

(with CH_3 included for comparison). The structural parameters and chemisorption energies are given in Table 1. Note that our calculation results are consistent with the work of Gong et al. [25]. An examination of Table 1 reveals two features. First, the distances between the unsaturated C atoms of n-alkyl groups ($n = 2$–6) and the nearest three Co atoms ($d_{C–Co}$) are almost the same, which implies that the bonding of these species with the Co surface is similar in these systems. This is in agreement with the fact that they have similar chemisorption energies. Second, the C–Co distances in CH_3 chemisorption are smaller than those of n-alkyl groups ($n = 2$–6). Thus, it is unsurprising that CH_3 has a greater chemisorption energy than the others (2.00 eV vs ∼1.60 eV). This may be because the repulsive interactions between the alkyl groups in n-alkyl groups ($n = 2$–6) and the surface are greater than those between H and the surface in CH_3.

Figs. 3a–3e illustrate the π-bound 1-alkenes on the top site, which are the most stable structures on Co(0001). Both of the two double-bond C atoms bind to the same Co atom, and the geometries are very similar to those on Ru(0001) reported by

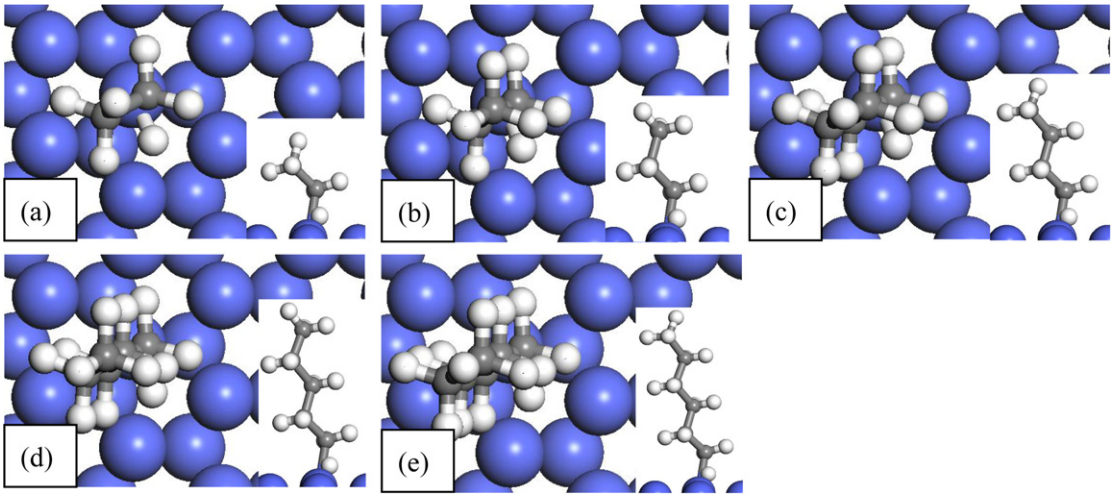

Fig. 4. Top view and side view (inserted) of the calculated TS structures of n-alkyl hydrogenation on Co(0001): (a) $CH_3CH_2 + H$; (b) $CH_3CH_2CH_2 + H$; (c) $CH_3(CH_2)_2CH_2 + H$; (d) $CH_3(CH_2)_3CH_2 + H$; (e) $CH_3(CH_2)_4CH_2 + H$.

Table 2
Structural parameters and DFT chemisorption energies of adsorbed 1-alkenes

Chain length n	$d_{C–Co}$ (Å)	Chem. energy (eV)
2	2.068, 2.080	0.96
3	2.093, 2.128	0.78
4	2.087, 2.130	0.78
5	2.084, 2.128	0.77
6	2.087, 2.123	0.79

$d_{C–Co}$ are the distances between the double-bond C atoms in 1-alkenes and the Co atom.

Table 3
Structural parameters at the TSs of n-alkyl hydrogenation on Co(0001)

Chain length n	$d_{C–Co}$ (Å)	$d_{H–Co}$ (Å)	$d_{C–H}$ (Å)
2	2.175	1.619, 1.912, 2.106	1.650
3	2.171	1.615, 1.884, 2.122	1.650
4	2.164	1.613, 1.907, 2.121	1.650
5	2.163	1.614, 1.905, 2.119	1.650
6	2.164	1.613, 1.908, 2.118	1.650

$d_{C–Co}$ is the distance between the unsaturated C atom and the Co atom. $d_{H–Co}$ are the distances between the reacting H atom and the nearest three Co atoms. $d_{C–H}$ is the distance between the reacting C and H atom.

Table 4
Barriers and chemisorption energies with different chain lengths

Chain length n	E_a^{hy}	E_a^{dehy}	E_a^{-dehy}	E_{ch}^{DFT}	$E_{ch}^{DFT} + E_a^{dehy} - E_a^{hy} - E_a^{-dehy}$
2	0.69	0.49	0.52	0.96	0.24
3	0.65	0.44	0.54	0.78	0.04
4	0.65	0.41	0.48	0.78	0.06
5	0.66	0.43	0.50	0.77	0.04
6	0.67	0.44	0.52	0.79	0.05

E_a^{hy} is the barrier of n-alkyl hydrogenation reaction. E_a^{dehy} and E_a^{-dehy} are the barrier of n-alkyl dehydrogenation reaction and its reverse reaction, respectively. E_{ch}^{DFT} is the chemisorption energy of 1-alkenes obtained from DFT calculations. The unit of energy is eV.

Ciobîcă et al. [45]. The structural parameters and chemisorption energies, given in Table 2, demonstrate that the distances ($d_{C–Co}$) between the double-bond C atoms and the Co atoms in ethylene chemisorption are smaller than those of the other 1-alkenes. This is similar to the chemisorption of n-alkyl groups possibly due to the same reason: the alkyl groups in 1-alkenes ($n = 2$–6) are more repulsed by the Co surface compared with H in ethylene. As a result, the chemisorption energy of ethylene is around 0.18 eV higher than of the other 1-alkenes.

3.2. Hydrogenation of n-alkyl groups

After obtaining the ISs, we located the TSs of n-alkyl hydrogenation. Fig. 4 illustrates the geometries of the TSs, and Table 3 gives some important structural parameters at the TSs. At the TSs, the n-alkyl groups move from the hcp hollow site to the top site, whereas the H atom is on the off-top site of the same Co atom on which the n-alkyl group sits. Although the chain length varies from 2 to 6, the main configurations of the TSs are the same. The distances between the reacting C and H ($d_{C–H}$) atom at the TSs are all about 1.65 Å, and the other structural parameters (Table 4) are also very similar. The barriers of these reactions are also similar, as shown in Table 4. Note that the calculated TSs of n-alkyl hydrogenation are very similar to those of CH_3 hydrogenation obtained by Gong et al. on Co(0001) [25], and by Ciobîcă et al. on Ru(0001) [46]; for example, Gong et al. calculated the distance between the reacting C and H atom as 1.621 Å, very similar to our finding of 1.65 Å.

3.3. Dehydrogenation of n-alkyl groups

After obtaining the barriers of hydrogenation of n-alkyl groups, we investigated the dehydrogenation of these species. We located the TSs of n-alkyl dehydrogenation; their geometries are displayed in Fig. 5, and some important structural parameters are given in Table 5. Fig. 5 shows that at the TSs, the two adsorbed C atoms bind to the same Co atom and the H atom is on the off-top site. The TS geometry is similar to that obtained by Neurock et al. on Pd(111) [47]. The main configurations of these TSs with different chain lengths also are the same. The data in Table 5 clearly show that the structural parameters at the TSs are almost identical except for C_2; for instance, the distances between the reacting C and H atom are

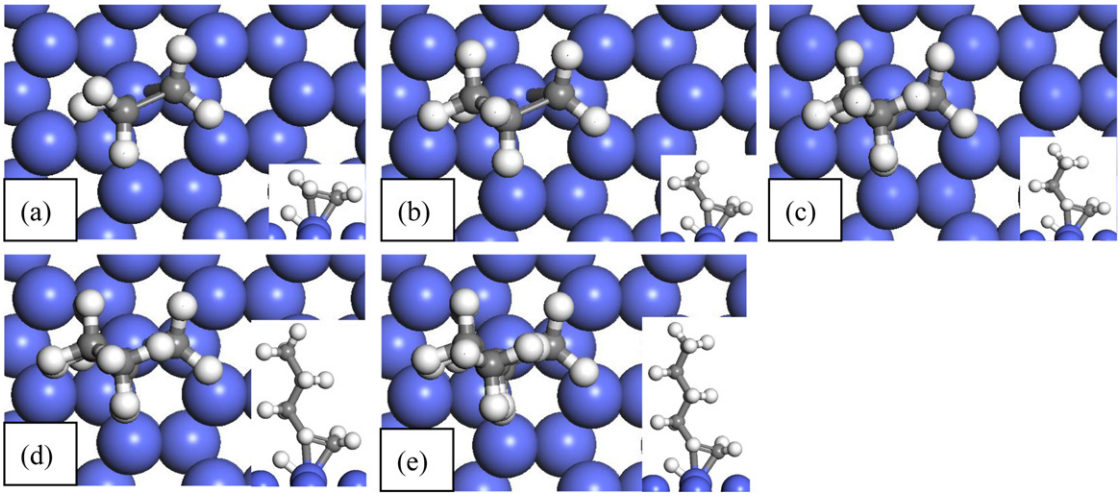

Fig. 5. Top view and side view (inserted) of the calculated TS structures of n-alkyl dehydrogenation (1-alkene hydrogenation) on Co(0001): (a) CH_3CH_2-H; (b) $CH_3CH_2CH_2-H$; (c) $CH_3(CH_2)_2CH_2-H$; (d) $CH_3(CH_2)_3CH_2-H$; (e) $CH_3(CH_2)_4CH_2-H$.

Table 5
Structural parameters at the TSs of n-alkyl dehydrogenation on Co(0001)

Chain length n	$d_{C–Co}$ (Å)	$d_{H–Co}$ (Å)	$d_{C–H}$ (Å)
2	2.078, 2.112	1.615, 1.918, 2.319	1.490
3	2.072, 2.141	1.645, 1.959, 2.264	1.550
4	2.075, 2.131	1.644, 1.950, 2.275	1.540
5	2.072, 2.137	1.646, 1.952, 2.257	1.560
6	2.073, 2.140	1.644, 1.951, 2.267	1.560

$d_{C–Co}$ are the distances between the double-bond C atoms and the Co atom. $d_{H–Co}$ are the distances between the reacting H atom and the nearest three Co atoms. $d_{C–H}$ is the distance between the reacting C and H atom.

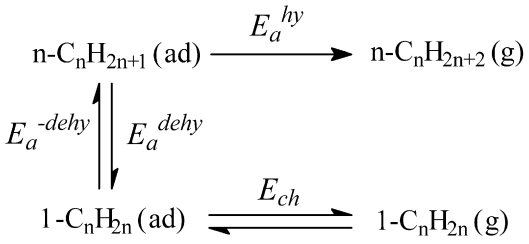

Fig. 6. Kinetic scheme of paraffin and α-olefin production. E_{ch} is the chemisorption energy of α-olefin. The other symbols are defined in the caption of Table 4.

all about 1.55 Å except that of C_2, which is 1.49 Å. Because n-alkyl hydrogenation and 1-alkene hydrogenation share the same TSs, we can estimate the barriers of both reactions based on the corresponding ISs. These barriers, given in Table 4, are very similar with different chain lengths due to their similar IS and TS geometries.

4. Discussion

4.1. Kinetic derivation of P/O ratio expression

To rationalize our calculation results, we propose a kinetic model, as shown in Fig. 6. The model is based on the general consensus that adsorbed n-alkyl groups (n-C_nH_{2n+1}) are hydrogenated to form n-alkanes (n-C_nH_{2n+2}), which desorb and cannot readsorb; that adsorbed 1-alkenes (1-C_nH_{2n}) are produced by dehydrogenation of n-alkyl and subsequently desorb to the gas phase; and that these two steps are reversible.

Based on this kinetic model, we derive an expression for the P/O ratio. Under typical reaction conditions, the desorption of paraffins is irreversible. Thus, the rate of paraffin formation, r_p (s^{-1}), can be given by

$$r_p = \frac{k_B T}{h} e^{-\frac{E_a^{hy}}{RT}} \theta_{C_nH_{2n+1}} \theta_H, \tag{2}$$

where k_B is the Boltzmann constant, h is the Planck's constant, T is temperature, R is gas constant, E_a^{hy} is the barrier of n-alkyl hydrogenation reaction, and $\theta_{C_nH_{2n+1}}$ and θ_H are the coverages of adsorbed n-alkyl group (n-C_nH_{2n+1}) and H, respectively.

At steady state, the rate of α-olefin formation is proportional to the partial pressure of the olefin and equal to $\frac{p_{C_nH_{2n}}}{p_{tot}} \times \nu$ (mol/s), where $p_{C_nH_{2n}}$ is the partial pressure of α-olefin (1-C_nH_{2n}), p_{tot} is the total pressure, and ν is the total flow rate (mol/s). The number of the total reactive sites is $A \times m$ (mol), where A is the total surface area of catalyst and m is the mol number of surface sites in a unit area of surface (mol/m^2). Thus, the rate of α-olefin formation, r_o (s^{-1}), can be written as

$$r_o = \frac{p_{C_nH_{2n}} \nu}{p_{tot} A m}. \tag{3}$$

Experimental work has shown that α-hydrogenation of n-alkyl groups is the slowest of the multistep hydrogenation reactions [20], which also is consistent with our DFT calculations. Thus, the preceding hydrogenation steps may reach quasi-equilibrium at steady state. Thus,

$$n\text{-}C_nH_{2n+1}(ad) + * \rightleftharpoons 1\text{-}C_nH_{2n}(ad) + H(ad),$$
$$\frac{\theta_{C_nH_{2n}} \theta_H}{\theta_{C_nH_{2n+1}} \theta_*} = e^{-\frac{E_a^{dehy} - E_a^{-dehy}}{RT}}, \tag{4}$$

where $\theta_{C_nH_{2n}}$ and θ_* are the coverages of adsorbed 1-C_nH_{2n} and surface free site, respectively, and E_a^{dehy} and E_a^{-dehy} are

the barriers of n-alkyl dehydrogenation reaction and its reverse reaction, respectively.

The desorption and readsorption of 1-C_nH_{2n} also may reach quasi-equilibrium, considering that surface reactions are much slower. Thus,[1]

$$\frac{\theta_{C_nH_{2n}}}{\frac{p_{C_nH_{2n}}}{p^o}\theta_*} = e^{\frac{E_{ch}+RT}{RT}+\frac{\Delta S^o}{R}}, \tag{5}$$

where p^o is the standard pressure (1 bar), E_{ch} is the chemisorption energy of α-olefin, and ΔS^o is the standard entropy difference between adsorbed (S^o_{ad}) and gaseous (S^o_g) α-olefin, which can be expressed by

$$\Delta S^o = S^o_{ad} - S^o_g. \tag{6}$$

Combining Eqs. (2)–(5), we can obtain the following equation to express the P/O ratio:

$$\ln\frac{r_p}{r_o} = \frac{E_{ch} + E_a^{dehy} - E_a^{hy} - E_a^{-dehy}}{RT} + \frac{\Delta S^o}{R} + \ln t, \tag{7}$$

where t is a constant with different chain lengths under certain reaction conditions, defined as

$$t = \frac{k_B T}{h}\frac{e p_{tot} A m}{p^o \nu}\theta_H^2. \tag{8}$$

The energy terms, such as E_a^{dehy}, E_a^{hy}, and E_a^{-dehy}, can be obtained from DFT calculations and are listed in Table 4. It is noteworthy that the chemisorption energy of α-olefin (E_{ch}^{DFT}) from our DFT calculations does not contain the van der Waals interaction between the adsorbate and the metal surface. To obtain the total chemisorption energy of the α-olefin (E_{ch}), our DFT calculation results should be corrected by including the van der Waals interaction (E_{ch}^{VDW}). Thus,

$$E_{ch} = E_{ch}^{DFT} + E_{ch}^{VDW}. \tag{9}$$

Taking Eq. (9), Eq. (7) can be rewritten as

$$\ln\frac{r_p}{r_o} = \frac{E_{ch}^{DFT} + E_a^{dehy} - E_a^{hy} - E_a^{-dehy}}{RT} + \frac{E_{ch}^{VDW} + T\Delta S^o}{RT} + \ln t. \tag{10}$$

It is noteworthy that Eq. (10) is exact except for the approximations mentioned above. Surface coverages of many intermediates, such as $\theta_{C_nH_{2n}}$ and $\theta_{C_nH_{2n+1}}$, are canceled in the derivation, and thus other elementary steps besides the steps in our kinetic model (Fig. 6) are not included.

4.2. Analysis of the terms in Eq. (10)

The value of the first energy term in Eq. (10), $E_{ch}^{DFT} + E_a^{dehy} - E_a^{hy} - E_a^{-dehy}$, for each chain length is given in Table 4. Two interesting features can be observed from the table: (i) For chain lengths $n > 2$, the values of $E_{ch}^{DFT} + E_a^{dehy} - E_a^{hy} - E_a^{-dehy}$ are almost the same and thus independent of the chain length, and (ii) the value of $E_{ch}^{DFT} + E_a^{dehy} - E_a^{hy} - E_a^{-dehy}$ of C_2 species is about 0.2 eV greater than that of the other chain lengths. These two features stem from the fact that the hydrogenation and dehydrogenation barriers (E_a^{dehy}, E_a^{hy}, and E_a^{-dehy}) are constant for different chain lengths, and the DFT chemisorption energies (E_{ch}^{DFT}) of α-olefins are independent of the chain length, except that the DFT chemisorption energy of ethylene is about 0.2 eV higher than that for the other α-olefins. Moreover, the third term in Eq. (10), $\ln t$, is also constant and independent of the chain length under the same reaction conditions. Thus, if only the first term and the third terms in Eq. (10) are considered, they are independent of the chain length except for C_2 species.

4.2.1. Van der Waals interaction between olefin and metal surface

The second term in Eq. (10),

$$\frac{E_{ch}^{VDW} + T\Delta S^o}{RT},$$

which contains the van der Waals interaction and entropy difference, is rather more complicated. Along with the direct chemical bonding, the van der Waals interaction between α-olefin and metal surface also contributes to the total chemisorption energy. Although the van der Waals interaction is not included in the exchange-correlation (XC) functional at the PBE level in the DFT framework, we can still estimate it from experimental work [48–53].

The weak bonding energy due to van der Waals forces can be measured experimentally by temperature-programmed desorption (TPD). Lavrich et al. [51] reported that the typical magnitude of the van der Waals interaction is about 6.1 kJ/mol per methylene (CH_2) subunit in saturated linear hydrocarbon chains adsorbed on Au(111). Sexton and Hughes found that a CH_2 group contributes 5–6.5 kJ/mol to the total bonding energy over Cu(100) and Pt(111) [53]. Dubois, Zegarski and Nuzzo estimated a methylene–surface interaction of ∼8 kJ/mol [48–50]. According to these experimental findings, it is reasonable to estimate that the van der Waals interaction energy between α-olefin and metal surface increases by 6–8 kJ/mol per CH_2 subunit; thus,

$$E_{ch}^{VDW} \propto c_1 n, \tag{11}$$

where c_1 is 6–8 kJ/mol.

4.2.2. Entropy difference between adsorbed and gaseous α-olefins

The total standard entropy of a gaseous molecule is a sum of contributions from translational, rotational, and vibrational modes. The number of vibrational modes is $3N - 5$ for a linear molecule and $3N - 6$ for a nonlinear molecule (where N is the number of atoms in the molecule). All of the vibrational modes can be obtained from DFT calculations. The contributions to entropy from translational and rotational modes can be calculated from the mass and the moments of inertia of the molecule [54,55]. Fig. 7a shows the total entropies of α-olefins in the gas

[1] The wax layer are not considered over the catalyst in the kinetic model, which means that the transportation of α-olefins in the wax is ignored.

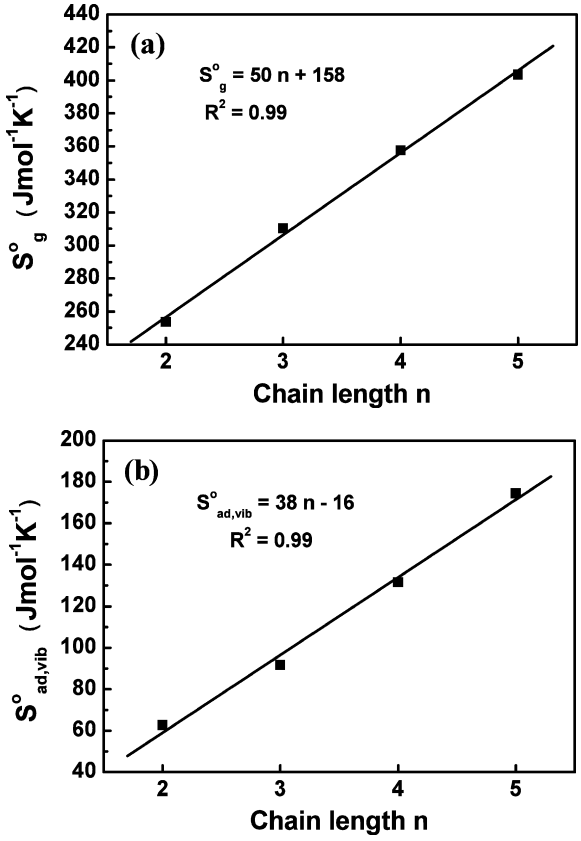

Fig. 7. (a) The entropy (S_g^o) of α-olefin in the gas phase as a function of the chain length n at 500 K. (b) The vibrational entropy ($S_{\mathrm{ad,vib}}^o$) of α-olefin on Co(0001) as a function of the chain length n at 500 K.

phase from C_2 to C_5 and plotted against chain length. A temperature of 500 K, the typical temperature under FT reaction conditions, was chosen. It is clear from Fig. 7a that the entropy of gaseous olefin is linear to the chain length, and that the linear function can be fitted into $S_g^o = 50n + 158$ ($\mathrm{J\,mol^{-1}\,K^{-1}}$).

In a molecule adsorbed on surfaces, translational and rotational modes are replaced by vibrational modes corresponding to frustrated translation and rotation. Then $3N-2$ vibrational modes arise, and the remaining 2 degrees of freedom account for two-dimensional frustrated translational modes on surfaces, which can be estimated from diffusion barrier based on the harmonic oscillation approximation [54,55]. The $3N-2$ vibrational frequencies of α-olefins on Co(0001) from C_2 to C_5 are given in Table 6. The vibrational entropies also were estimated at 500 K and plotted against the chain length, as shown in Fig. 7b. This figure shows that the vibrational entropy is a linear function of chain length; curve fitting gives rise to $S_{\mathrm{ad,vib}}^o = 38n - 16$ ($\mathrm{J\,mol^{-1}\,K^{-1}}$). Regarding the other two modes of surface diffusion, their contributions to the entropy are rather smaller compared with those from the vibrational modes; for example, a diffusion barrier of 0.10 eV may lead to an entropic contribution of $\sim$20 $\mathrm{J\,mol^{-1}\,K^{-1}}$. More importantly, the entropic contribution from the two frustrated translational modes changes very little with chain length. Thus, compared with the strong dependence of the vibrational entropy on chain length, the variation of the translational entropy of α-olefins with different chain lengths can be neglected.

Table 6
Calculated vibrational frequencies of adsorbed α-olefins from C_2 to C_5

Chain length n	Frequencies ($\mathrm{cm^{-1}}$)
2	51, 306, 412, 607, 752, 765, 825, 855, 1109, 1119, 1310, 1384, 2969, 2982, 3048, 3072
3	135, 176, 219, 314, 362, 409, 670, 792, 847, 894, 948, 979, 1100, 1120, 1233, 1281, 1328, 1354, 1365, 2650, 2906, 2907, 2949, 2993, 3021
4	73, 135, 152, 215, 231, 352, 375, 505, 677, 722, 793, 832, 927, 958, 991, 1027, 1098, 1122, 1172, 1225, 1251, 1299, 1340, 1350, 1378, 1386, 2597, 2876, 2922, 2941, 2942, 2974, 3032, 3040
5	55, 74, 115, 157, 188, 230, 308, 353, 386, 523, 672, 689, 788, 818, 856, 895, 963, 996, 1042, 1058, 1101, 1121, 1155, 1195, 1227, 1241, 1284, 1315, 1343, 1351, 1374, 1385, 1393, 2581, 2882, 2916, 2935, 2937, 2941, 2967, 2991, 3029, 3041

Based on the foregoing analyses on the entropies of gaseous and adsorbed α-olefins, we can state the following relationship between the entropy difference and the chain length from Eq. (6) [$S_g^o = 50n+158$ and $S_{\mathrm{ad,vib}}^o = 38n-16$ ($\mathrm{J\,mol^{-1}\,K^{-1}}$)]:

$$\Delta S^o \propto -12n, \tag{12}$$

where the unit of ΔS^o is $\mathrm{J\,mol^{-1}\,K^{-1}}$. At 500 K, the $T\Delta S^o$ of the α-olefin decreases by 6 kJ/mol per CH_2 subunit.

Combining Eqs. (11) and (12), we can obtain that the second term in Eq. (10), $\frac{E_{\mathrm{ch}}^{\mathrm{VDW}}+T\Delta S^o}{RT}$, is linearly dependent of the chain length,

$$\frac{E_{\mathrm{ch}}^{\mathrm{VDW}}+T\Delta S^o}{RT} \propto cn, \tag{13}$$

where the slope c is 0–0.48, estimated from Eqs. (11) and (12).

We also calculated the zero-point energies (ZPEs) of the gaseous and adsorbed α-olefins from their vibrational frequencies. We found that the ZPE differences between the gaseous and adsorbed α-olefins were all <0.02 eV from C_2 to C_5. Thus, the ZPE differences are neglectable.

4.3. General discussion

4.3.1. Chain length dependence of P/O ratio

On the basis of the foregoing analyses, the chain length dependence of the P/O ratio shown in Fig. 1 can be explained by examining the three terms in Eq. (10). The third term, $\ln t$, is constant for all the chain lengths under the same conditions. The second term,

$$\frac{E_{\mathrm{ch}}^{\mathrm{VDW}}+T\Delta S^o}{RT},$$

is a linear function of the chain length with a slope of 0–0.48. In the first term, the values of $E_{\mathrm{ch}}^{\mathrm{DFT}} + E_a^{\mathrm{dehy}} - E_a^{\mathrm{hy}} - E_a^{-\mathrm{dehy}}$ are the same for all of the chain lengths except C_2; therefore, when the chain length $n > 2$, the first term and third term in Eq. (10) are constant, and the P/O ratio is determined just by

$$\frac{E_{\mathrm{ch}}^{\mathrm{VDW}}+T\Delta S^o}{RT},$$

causing ln(P/O) to be linearly dependent of the chain length. As for C_2, the greater value of $E_{ch}^{DFT} + E_a^{dehy} - E_a^{hy} - E_a^{-dehy}$ (about 0.2 eV higher than those with chain lengths $n > 2$) results in the higher ethane/ethylene ratio.

Moreover, Eq. (10) can be simplified exactly to Eq. (1) obtained from experimental observations [33] after C_2. The slope c obtained from experimental work [30,33], which may change slightly with changing reaction conditions, is in the range of 0.3–0.5. From this work, the slope c is 0–0.48, which is consistent with the experimental result. It is noteworthy that the slope in this work is determined by our first principles calculations, except for the estimation of van der Waals interaction, which comes from experimental work.

As mentioned in the Introduction, previous authors have proposed chain length-dependent solubility [34,35], diffusivity [36–38] and physisorption [31] to explain the chain length dependence of the P/O ratio. For the first two explanations, a wax layer over the catalyst surface is essential in the kinetic models. Our current work demonstrates the dependence even without the liquid phase, which is consistent with the experimental work [31], suggesting that these two factors may not be the physical origin of the chain length dependence of the P/O ratio, but still may have some affect on the chain length dependence of the P/O ratio, because varied dependences often were found under different reaction conditions [3,18,31,36–38]. For example, Geerlings et al. [3] suggested that the chain length dependence of the P/O ratio is related to the desorption energies of paraffin and olefin from the liquid phase to the gas phase. The chain length dependence of the desorption energy is stronger under conditions of dry operation (without the wax layer) than in the presence of the liquid phase [3].

Regarding the physisorption model, Kuipers et al. [31,32] proposed that physisorption acts as an umbilical cord between the α-olefin and the growth site. Schulz et al. [18] argued that this scenario could suggest a transportation limitation, which would lead to a preferred reinsertion of indigenous olefins as opposed to the insertion of cofed olefins. However, with the cofeeding of α-olefin of different chain lengths in a slurry reactor, Schulz et al. [18] found no evidence of severe transportation limitations. In our kinetic analysis, the α-olefins chemisorbed on the metal surface are assumed to reach quasi-equilibrium with those in the gas phase [see Eq. (5)]; thus, in the transportation processes among the physisorption layer, the liquid phase and the gas phase are not limiting steps. Note the similarity between our model and the physisorption model. The physisorption is the van der Waals interaction in nature, whereas our work shows that the van der Waals interaction, as a part of the chemisorption energy (E_{ch}^{VDW}), is an element leading to the chain length dependence of the P/O ratio.

Differences between our model and the physisorption model also are apparent. In our model, the transportation limitation is not a factor causing chain length dependence, whereas transportation limitation is the key factor in the physisorption model. In other words, the absence of the physisorption layer or the liquid phase still can result in the chain length dependence in our model. Also in our model, the van der Waals interaction and entropy difference (ΔS^o) are identified as the physical origin of the chain length dependence of the P/O ratio.

4.3.2. Implications

Equation (10) provides other information besides explaining, for the first time, the simultaneous erratic behavior of C_2 and exponential increase in the P/O ratio for other chain lengths. Although the third term, $\ln t$, is constant with different chain lengths, the reaction conditions can change this value [see Eq. (8)]; for example, increasing the H_2 partial pressure will increase θ_H, leading to a higher t and P/O ratio, whereas increasing the CO partial pressure will enhance CO dissociation and increase surface coverage of carbon species, giving rise to a lower θ_H and greater olefin selectivity. Decreasing the flow rate v and increasing the surface area A will improve the paraffin selectivity. This understanding obtained from Eq. (10) is in good agreement with the experimental findings [18,31].

Equation (10) also provides some hints how to promote the catalysts to improve the α-olefin selectivity. As discussed earlier, the strong bonding of ethylene on catalyst surfaces gives rise to low α-olefin selectivity for C_2, suggesting that weakening of olefin–surface bonds will facilitate desorption of olefins and enhance α-olefin selectivity. For instance, when doping some promoters that can reduce the α-olefin chemisorption, the α-olefin selectivity will be improved. It should be mentioned that modifying surface reactivity by promoters can greatly change the chemisorption energies, and yet the surface reaction barriers [i.e., E_a^{dehy}, E_a^{hy} and E_a^{-dehy} in Eq. (10)] will not be significantly altered, because the energies of ISs and TSs on surfaces usually increase or decrease simultaneously. Therefore, the chemisorption energy of the α-olefin may be a very good controlling parameter in determining α-olefin selectivity in FT synthesis.

5. Conclusion

Having performed extensive DFT calculations and kinetic analyses, we are now in a position to explain the chain length dependence of the P/O ratio in FT synthesis. The following conclusions can be stated:

(i) The geometries of adsorbed n-alkyl groups on Co(0001) are similar. Methyl has greater chemisorption energy than the others (∼2.0 eV vs ∼1.6 eV). Adsorbed 1-alkenes also have similar geometries on Co(0001) with two double-bond C atoms sitting on the top site. The chemisorption energy of ethylene is 0.96 eV, larger than that of the others (∼0.78 eV).

(ii) All of the TS geometries of n-alkyl hydrogenation are similar with different chain lengths. The distances between the reacting C and H atoms are all about 1.6 Å, and the barriers are similar as well (0.65–0.69 eV). All of the TS geometries of n-alkyl dehydrogenation also are very similar. The distances between the reacting C and H atoms are about 1.5 Å. The barriers of the forward and reverse reactions of n-alkyl dehydrogenation with different chain lengths are very similar.

(iii) The chain length dependence of the P/O ratio is attributed to the linear relationship of the van der Waals interaction between adsorbed olefins and metal surfaces and the entropy difference between adsorbed and gaseous olefins on the chain length [see the second term in Eq. (10)]. The greater chemisorption energy of ethylene compared with that of the other 1-alkenes results in the anomaly of the ethane/ethylene ratio.

Acknowledgments

The authors thank The Queen's University of Belfast for computing time. J.C. acknowledges Johnson Matthey for financial support.

References

[1] (a) F. Fischer, H. Tropsch, Brennst. Chem. 4 (1923) 276;
(b) F. Fischer, H. Tropsch, Brennst. Chem. 7 (1926) 79;
(c) F. Fischer, H. Tropsch, Chem. Ber. 59 (1926) 830.
[2] H. Schulz, Appl. Catal. A 186 (1999) 3.
[3] J.J.C. Geerlings, J.H. Wilson, G.J. Kramer, H.P.C.E. Kuipers, A. Hoek, H.M. Huisman, Appl. Catal. A 186 (1999) 27.
[4] P. Biloen, W.M.H. Sachtler, Adv. Catal. 30 (1981) 165.
[5] C.K. Rofer-Depoorter, Chem. Rev. 81 (1981) 447.
[6] E. Iglesia, Appl. Catal. A 161 (1997) 59.
[7] M.E. Dry, Appl. Catal. A 138 (1996) 319.
[8] M.E. Dry, Catal. Today 71 (2002) 227.
[9] R.A. Dictor, A.T. Bell, J. Catal. 97 (1986) 121.
[10] J.G. Ekerdt, A.T. Bell, J. Catal. 62 (1980) 19.
[11] K.R. Krishna, A.T. Bell, J. Catal. 139 (1993) 104.
[12] T. Komaya, A.T. Bell, J. Catal. 146 (1994) 237.
[13] P.M. Maitlis, R. Quyoum, H.C. Long, M.L. Turner, Appl. Catal. A 186 (1999) 363.
[14] M.L. Turner, P.K. Byers, H.C. Long, P.M. Maitlis, J. Am. Chem. Soc. 115 (1993) 4417.
[15] M.L. Tuner, N. Marsih, B.E. Man, R. Quyoum, H.C. Long, P.M. Maitlis, J. Am. Chem. Soc. 124 (2002) 10456.
[16] (a) J.F. Kummer, P.H. Emmett, J. Am. Chem. Soc. 75 (1953) 5177;
(b) H. Pichler, H. Schulz, Chem. Ing. Tech. 12 (1970) 1160.
[17] (a) R. Brady, R. Pettit, J. Am. Chem. Soc. 102 (1980) 6181;
(b) R. Brady, R. Pettit, J. Am. Chem. Soc. 103 (1981) 1287.
[18] (a) H. Schulz, M. Claeys, Appl. Catal. A 186 (1999) 71;
(b) H. Schulz, M. Claeys, Appl. Catal. A 186 (1999) 91;
(c) E. van Steen, H. Schulz, Appl. Catal. A 186 (1999) 309.
[19] C.A. Mims, L.E. McCandlish, J. Phys. Chem. 91 (1987) 929.
[20] (a) J.J.C. Geerlings, M.C. Zonnevylle, C.P.M. de Groot, Surf. Sci. 241 (1991) 302;
(b) J.J.C. Geerlings, M.C. Zonnevylle, C.P.M. de Groot, Surf. Sci. 241 (1991) 315.
[21] J. Panpranot, J.G. Goodwin Jr., A. Sayari, J. Catal. 213 (2003) 78.
[22] S. Li, G.D. Meitzner, E. Iglesia, J. Phys. Chem. B 105 (2001) 5743.
[23] Z.-P. Liu, P. Hu, J. Am. Chem. Soc. 124 (2002) 11568.
[24] X.-Q. Gong, R. Raval, P. Hu, Surf. Sci. 562 (2004) 247.
[25] X.-Q. Gong, R. Raval, P. Hu, J. Chem. Phys. 122 (2005) 024711.
[26] I.M. Ciobîcă, F. Frechard, R.A. van Santen, A.W. Kleyn, J. Hafner, Chem. Phys. Lett. 311 (1999) 185.
[27] I.M. Ciobîcă, G.J. Kramer, Q. Ge, M. Neurock, R.A. van Santen, J. Catal. 212 (2002) 136.
[28] I.M. Ciobîcă, F. Frechard, A.P.J. Jansen, R.A. van Santen, Stud. Surf. Sci. 133 (2001) 221.
[29] S.L. Soled, E. Iglesia, S. Miseo, B.A. Derites, R.A. Fiato, Top. Catal. 2 (1995) 193.
[30] E. Iglesia, S.C. Reyes, R.J. Madon, J. Catal. 129 (1991) 238.
[31] E.W. Kuipers, I.H. Vinkenburg, H. Oosterbeek, J. Catal. 152 (1995) 137.
[32] E.W. Kuipers, C. Scheper, J.H. Wilson, I.H. Vinkenburg, H. Oosterbeek, J. Catal. 158 (1996) 288.
[33] B. Shi, B.H. Davis, Catal. Today 106 (2005) 129.
[34] L.M. Tau, H.A. Dabbagh, B.H. Davis, Energy Fuels 4 (1990) 94.
[35] H. Schulz, K. Beck, E. Erich, in: D.M. Bibby, C.D. Chang, R.F. Howe, S. Yurchak (Eds.), Studies in Surface, Science and Catalysis, vol. 36, Elsevier, Amsterdam, 1988, p. 457.
[36] R.J. Madon, S.C. Reyes, E. Iglesia, J. Phys. Chem. 4 (1991) 7795.
[37] R.J. Madon, E. Iglesia, J. Catal. 139 (1993) 576.
[38] E. Iglesia, S.C. Reyes, R.J. Madon, S.L. Soled, Adv. Catal. 39 (1993) 221.
[39] J.M. Soler, E. Artacho, J.D. Gale, A. García, J. Junquera, P. Ordejón, D. Sánchez-Portal, J. Phys. Condens. Matter 14 (2002) 2745.
[40] N. Troullier, J.L. Martins, Phys. Rev. B 43 (1991) 1993.
[41] J.P. Perdew, K. Burke, M. Ernzerhof, Phys. Rev. Lett. 77 (1996) 3865.
[42] A. Alavi, P. Hu, T. Deutsch, P.L. Silvestrelli, J. Hutter, Phys. Rev. Lett. 80 (1998) 3650.
[43] C.-J. Chang, P. Hu, J. Am. Chem. Soc. 122 (2000) 2134.
[44] C.-J. Chang, P. Hu, A. Alavi, J. Am. Chem. Soc. 121 (1999) 7931.
[45] I.M. Ciobîcă, The molecular basis of the Fischer–Tropsch reaction, Ph.D. thesis.
[46] I.M. Ciobîcă, F. Frechard, R.A. van Santen, A.W. Wleyn, J. Hafner, J. Phys. Chem. 104 (2000) 3364.
[47] M. Neurock, V. Pallassana, R.A. van Santen, J. Am. Chem. Soc. 1 (2000) 1150.
[48] L.H. Dubois, B.R. Zegarski, R.G. Nuzzo, J. Chem. Phys. 98 (1993) 678.
[49] R.G. Nuzzo, B.R. Zegarski, L.H. Dubois, J. Am. Chem. Soc. 109 (1987) 733.
[50] L.H. Dubois, B.R. Zegarski, R.G. Nuzzo, J. Am. Chem. Soc. 112 (1990) 570.
[51] D.J. Lavrich, S.M. Wetterer, S.L. Bernasek, G. Scoles, J. Phys. Chem. B 102 (1998) 3456.
[52] L. Salem, J. Chem. Phys. 37 (1962) 2100.
[53] B.A. Sexton, A.E. Hughes, Surf. Sci. 140 (1984) 227.
[54] R.D. Cortright, J.A. Dumesic, Adv. Catal. 46 (2001) 161.
[55] A.A. Gokhale, S. Kandoi, J.P. Greeley, M. Mavrikakis, J.A. Dumesic, Chem. Eng. Sci. 59 (2004) 4679.